Ruthenium(II) and Ruthenium(III) Complexes Containing the $[pyS_4]^{2-}$ Ligand [pyS_4^{2-} = 2,6-Bis(2-mercaptophenylthio)dimethylpyridine(2−)][‡]

Dieter Sellmann,[†][a] Kinga Hein,*[a] and Frank W. Heinemann[a]

Keywords: Ruthenium / S ligands / Oxidation reactions

In the search for complexes, having sulfur-dominated coordination spheres, that potentially bind, activate, or stabilize nitrogenase-relevant small molecules, we have synthesized several ruthenium–sulfur complexes of the type $[Ru(L)(pyS_4)]$ starting from the labile acetonitrile complex $[Ru(NCMe)(pyS_4)]$ (**2**). Complex **2** was obtained from the reduction of $[Ru(NO)(pyS_4)]Br$ (**1**) by $N_2H_4{\cdot}H_2O$ in the presence of MeCN. The acetonitrile ligand in **2** could be exchanged for the soft σ–π ligand CO to give $[Ru(CO)(pyS_4)]$ (**3**). Attempts to coordinate N_2 to the pyS_4^{2-} fragment of **2** gave $[\{Ru(pyS_4)\}_2]$ (**4**). Complex **2** reacts also with hard σ-ligands, such as N_2H_4, NH_3, pyridine, and pyrazine, to afford mononuclear $[Ru(N_2H_4)(pyS_4)]$ (**5**), $[Ru(NH_3)(pyS_4)]$ (**6**), $[Ru(py)(pyS_4)]$ (**7**), and $[Ru(pyr)(pyS_4)]$ (**8**), respectively. Reaction of **2** with NEt_4N_3 resulted in the formation of $NEt_4[Ru(N_3)(pyS_4)]$ (**9**). The oxidation of **2** with I_2 afforded $[Ru(I)(pyS_4)]$ (**10**). The protonated and alkylated species $[Ru(NCMe)(pyS_4\text{-}H)]BF_4$ (**11**), $[Ru(NCMe)(pyS_4\text{-}Et)]BF_4$ (**12**), and $[\{Ru(pyS_4\text{-}Et)\}_2](BF_4)_2$ (**13**) were obtained from **2** by its treatment with HBF_4 or Et_3OBF_4. The N_2H_4 ligand in **5** could not be oxidized to N_2H_2: the oxidation of the Ru^{II} center to Ru^{III} takes place instead. Attempts to oxidize **5** using either $[FeCp_2]PF_6$ or I_2 gave $[\{Ru^{II/III}(pyS_4)\}_2](PF_6)$ (**14**) and $[Ru^{III}(NH_3)(pyS_4)]X$ (X = PF_6, I) (**15**, **16**). The oxidation of **3** and **6** by $NOBF_4$ gave Ru^{III} species of $[Ru^{III}(CO)(pyS_4)]BF_4$ (**17**) and $[Ru^{III}(NH_3)(pyS_4)]BF_4$ (**18**). The oxidation of **5** and **6** with H_2O_2 afforded $[\{Ru^{II}(pyS_4{-}O_3)\}_2]$ (**19**), $[\{Ru^{II}(pyS_4{-}O_4)\}_2]$ (**20**) and $[Ru^{II}(NH_3)(pyS_4{-}O_4)]$ (**21**). All complexes were characterized by spectroscopic methods and by elemental analysis. The molecular structures of **4**, **6**, **10**, **14**, **15**, **19**, and **20** were determined by X-ray crystallographic analyses.

Introduction

Transition metals in sulfur-dominated coordination spheres exhibit rich coordination chemistry.[1] Sulfur coordination of transition metals is characteristic of the active sites of metal sulfur oxidoreductases, such as nitrogenases[2] and the nitrile hydratase.[3] To create model compounds, different multidentate organosulfur ligands and their transition metal complexes have been synthesized and investigated.[4] The previously reported $[M(N_HS_4)]$ fragment [$N_HS_4^{2-}$ = 2,2′-bis(2-mercaptophenylthio)diethylamine-(2−)] binds a number of nitrogenase-relevant molecules, such as CO, NO, N_2H_2, N_2H_4, and NH_3, but with the exception of N_2.[5] Moreover, in the case of ruthenium, the diastereoisomerism of the $[M(N_HS_4)]$ fragments leads to the formation of inseparable mixtures of $[Ru(L)(N_HS_4)]$ species. To overcome this problem, the flexible $N(C_2H_4)_2$ bridge was replaced by the rigid $py(CH_2Br)_2$ bridge, which yielded exclusively *trans*-alkylated species. The synthesis of many iron,[6,7c,7e] but only a few ruthenium complexes containing the $[M(pyS_4)]$ fragment have been described.[7a,7b] The extreme lability of important nitrogenase-relevant intermediates, such as $[Fe(N_2H_4)(pyS_4)]$ and $[\mu\text{-}N_2H_2\{Fe(pyS_4)\}_2]$,[8] prompted us to examine the coordination behavior of the pyS_4 ligand towards ruthenium − a homologue of the nitrogenase-dominating iron systems. In the case of ruthenium, the syntheses of $[Ru(L)(pyS_4)]$ complexes, e.g., $[Ru(CO)(pyS_4)]$, require very drastic conditions.[7a] The previous reports have also illustrated the difficulties in finding complexes with labile ligands L. Therefore, our primary aim was to find $[Ru(L)(pyS_4)]$ complexes with labile ligands which are capable of coordinating nitrogenase-relevant small molecules under mild conditions. In this context, we investigated the chemistry of $[Ru(L)(pyS_4)]$ complexes. Herein, we describe the synthesis of labile $[Ru(NCMe)(pyS_4)]$ (**2**) and its reactivity towards various nitrogenase-relevant molecules, such as CO and N_2H_4. We prove also the possibility of coordinating the σ ligands NH_3 and N_3^- to the $[Ru(pyS_4)]$ fragment; these ligands do not coordinate to the Fe analogue.[8] Attempts to oxidize coordinated hydrazine to diazene units led either to the oxidation of Ru^{II} to Ru^{III} or to the oxidation of thiolate donors in the pyS_4 ligand to sulfinates/sulfenates. This is a new observation when compared to the behavior

[‡] Transition Metal Complexes with Sulfur Ligands, 164. Part 163: D. Sellmann, R. Prakash, F. W. Heinemann, M. Moll, M. Klimowicz, *Angew. Chem. Int. Ed.* **2004**, *43*, 1877−1880.

[†] Deceased.

[a] Institut für Anorganische Chemie der Universität Erlangen-Nürnberg,
Egerlandstraße 1, 91058 Erlangen, Germany
Fax: (internat.) + 49-(0)9131-8527367
E-mail: kinga@anorganik.chemie.uni-erlangen.de

  DOI: 10.1002/ejic.200400066

of other ruthenium sulfur hydrazine complexes, such as $[Ru(N_2H_4)(PPh_3)(tpS_4)]$,[9] $[Ru(N_2H_4)(P\mathit{i}Pr_3)(S_4)]$, $[Ru(N_2H_4)(PCy_3)(S_4)]$,[10] and $[Ru(N_2H_4)(PPh_3)(^{bu}S_4)]$.[11]

Results

Earlier attempts to synthesize the acetonitrile complex **2** directly from $[RuCl_2(CH_3CN)_4]$ and Li_2pyS_4 were unsuccessful.[7a] Now, we have found that **2** can be synthesized from $[Ru(NO)(pyS_4)]Br$ (**1**) by reductive elimination of the NO^+ ligand. Treatment of **1** with two equiv. of $N_2H_4{\cdot}H_2O$ in acetonitrile afforded the target complex **2** (Scheme 1).

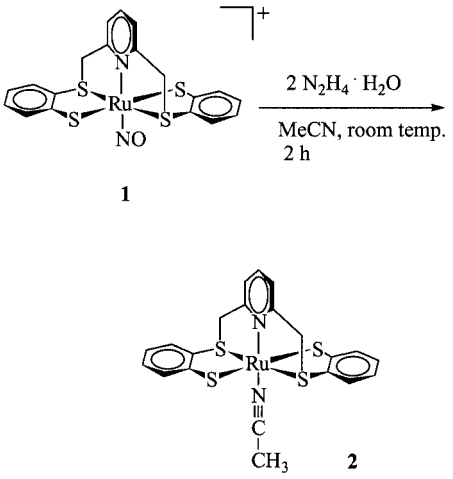

Scheme 1. Synthesis of $[Ru(NCMe)(pyS_4)]$ (**2**)

The NO^+ ligand in **1** is reduced by $N_2H_4{\cdot}H_2O$, giving probably the highly reactive and unstable 19-VE $[Ru(NO)(pyS_4)]^0$ intermediate, which releases NO and coordinates MeCN to afford **2**. The acetonitrile complex **2** is soluble in CH_2Cl_2 and THF, but it is insoluble in MeOH and Et_2O. ^1H and ^{13}C NMR spectra indicate that **2** exhibits C_2 symmetry in solution. In the solid state, **2** can be stored at room temp. for a couple of weeks, but it decomposes in solution over the course of 48 h. Complex **2** is an excellent starting material for the synthesis of numerous complexes that had been inaccessible previously. The reactivity of **2** towards various nucleophiles is depicted in Scheme 2.

Complex **2** reacts with CO instantaneously to give the CO complex **3**; this process indicates the lability of **2**. Attempts to exchange the acetonitrile ligand in **2** by N_2 led to the formation of the stable, dinuclear $[\{Ru(pyS_4)\}_2]$ (**4**). Complex **4** could be obtained in better yield when **2** was heated under reflux in THF for a few days. When **2** was treated with $N_2H_4{\cdot}H_2O$, a mononuclear hydrazine complex formed: $[Ru(N_2H_4)(pyS_4)]$ (**5**). Complex **5** is stable in solution for only a few hours and all attempts to obtain single crystals suitable for X-ray analysis resulted in the formation of crystals of **4**. Although one of the decomposition products of **5** was identified as $[Ru(NH_3)(pyS_4)]$ (**6**), formation of an N_2H_2 complex, resulting from disproportionation, has never been observed. Attempts to synthesize a diazene complex directly from **2** and N_2H_2, generated in situ by hydrolysis of $K_2N_2(CO_2)_2$ with acetic acid, were unsuccessful. Complex **6** could be prepared very simply from **2** in a reaction with gaseous NH_3 under ambient conditions. In contrast to the $[Fe(pyS_4)]$ fragment, which does not coordinate

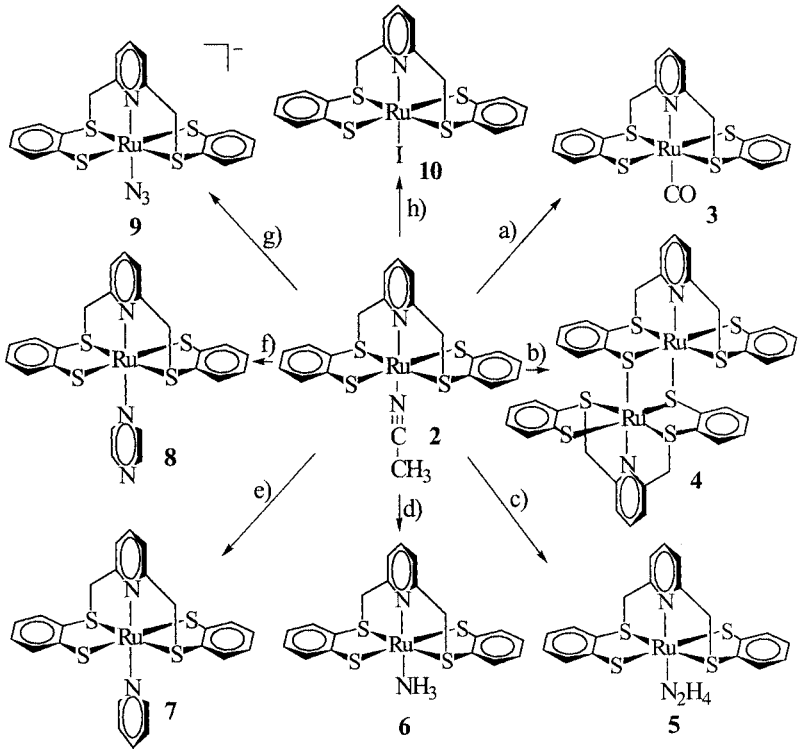

Scheme 2. Reactivity of **2** towards nitrogenase-relevant molecules: a) CO, THF, room temp.; b) N_2, THF, 100 bar; c) $N_2H_4{\cdot}H_2O$, THF, 15 h, room temp.; d) NH_3(g), THF, 2 h, room temp.; e) pyridine, 5 min, reflux; f) pyrazine, 15 min, reflux; g) NEt_4N_3, acetone, 50 °C; h) 0.5 I_2, THF, 30 min, room temp.

σ ligands at all, the NH_3 ligand in **6** proved to be very inert. The CO exchange reaction takes place very slowly and requires ca. 72 h to reach completion. For that reason, **6** did not afford a dinitrogen complex either. Attempts to exchange NH_3 for N_2 were unsuccessful, even under very drastic conditions, e.g., 100 bar/50 °C. Treatment of **2** with other hard σ ligands, such as pyridine and pyrazine, led to the formation of [Ru(py)(pyS_4)] (**7**) and [Ru(pyr)(pyS_4)] (**8**), respectively. To drive the reactions to completion, the solutions were usually heated under reflux for a short period of time. Azide complexes are used for the preparation of dinitrogen complexes that are not accessible by direct coordination of gaseous nitrogen.[12] Treatment of **2** in acetone with NEt_4N_3 afforded the extremely unstable azide complex NEt_4[Ru(N_3)(pyS_4)] (**9**) whose formation can be ascertained only by IR spectroscopy, which shows a characteristic ν(N_3) absorption at 2026 cm^{-1}. This absorption is in good agreement with those of other [Ru(N_3)(L)]$^-$ complexes, e.g., NEt_4[Ru(N_3)(PPh_3)(tpS_4)] (2029 cm^{-1}),[9] NEt_4[Ru(N_3)(PPh_3)($^{bu}S_4$)] (2034 cm^{-1}),[11] and NEt_4[Ru(N_3)(PCy_3)(S_4)] (2028 cm^{-1}).[13] This reaction took place only when the mixture was heated briefly at 50 °C. The azide complex proved to be too labile to obtain reasonable ^{1}H NMR spectra, and elemental analysis proved also to be very erratic. This situation most certainly is due to the inherent instability of the azide ligand, which proved to be very labile: the compound decomposed when it was dried in vacuo.

Oxidation of **2** with 0.5 equiv. of I_2 in THF led to a color change from orange-red to violet. Addition of *n*-hexane to the filtrate precipitated a violet solid, which we characterized by elemental analysis, mass spectrometry, and X-ray crystallography to be [Ru(I)(pyS_4)] (**10**). Addition of an excess of I_2 to a filtrate after preparation of **10** led to the formation of single crystals, which we identified with the help of an X-ray analysis to be [Ru^{III}(pyS_4)]$_2$(I_3)$_2$ (**22**). In the presence of an excess of iodine, the iodide ligand in **10** dissociates in solution and then two [Ru(pyS_4)] fragments dimerize to form **22**.

We performed protonation and alkylation experiments to further explore the reactivity of [Ru(NCMe)(pyS_4)] (**2**). When **2** was treated with 1 equiv. of HBF_4 at −78 °C, the protonated [Ru(NCMe)(pyS_4-H)]BF_4 (**11**) complex formed; it has a characteristic ν(CN) absorption at 2273 cm^{-1}. Addition of 1 equiv. of Et_3OBF_4 to **2** led to the formation of the monoalkylated species [Ru(NCMe)(pyS_4-Et)]BF_4 (**12**), which has a ν(CN) frequency at 2282 cm^{-1}. To prove the possibility that **2** can be dialkylated, we added an excess (5 equiv.) of Et_3OBF_4 to **2**. In the course of 2 days, the dinuclear complex [{Ru(pyS_4-Et)}$_2$](BF_4)$_2$ (**13**) formed. These observations regarding the reactivity of the [Ru(pyS_4)] acetonitrile complex confirm its wide applicability to the synthesis of other [Ru(L)(pyS_4)] complexes, but only when the entering ligand L is competitive enough to form the desired [Ru(L)(pyS_4)] species.

Our unsuccessful attempts to obtain a [Ru(pyS_4)] dinitrogen complex from its acetonitrile, ammonia, or azide precursors prompted us to return to the hydrazine complex **5** as a starting point. The oxidation of **5** by other oxidants gave unexpected, but interesting, results, which are summarized in Scheme 3.

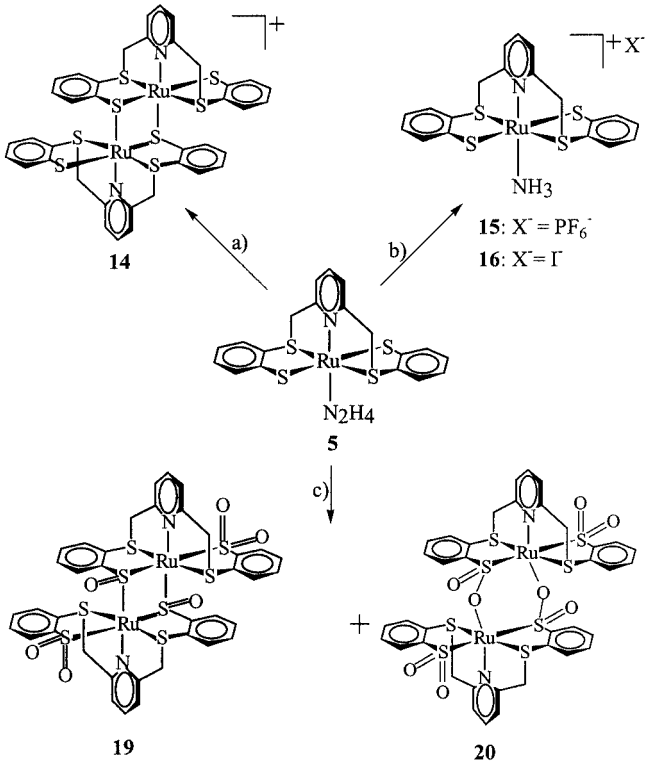

Scheme 3. Oxidation of [Ru(N_2H_4)(pyS_4)] (**5**) with different oxidants: a) [$FeCp_2$]PF_6, LiOMe; b) [$FeCp_2$]PF_6 or I_2; c) H_2O_2

When **5** was treated with 2 equiv. of [$FeCp_2$]PF_6 and 1 equiv. of LiOMe, red microcrystals formed which were identified as **4**. The red solid that precipitated from the filtrate, upon the addition of Et_2O, was separated and characterized as [{$Ru^{II/III}$(pyS_4)}$_2$](PF_6) (**14**). The hydrazine ligand in **5** dissociates in solution and then the resulting two [Ru(pyS_4)] fragments dimerize to form **4**. Overnight, a slow oxidation of the metal centers took place in the mother liquor to produce the mixed-valence species **14**. Treatment of **5** with an excess of either [$FeCp_2$]PF_6 or I_2 gave [Ru^{III}(NH_3)(pyS_4)]X (X = PF_6, I) (**15**, **16**). To gain some understanding of the formation of these stable ammonia complexes (**15**, **16**), we performed some additional oxidation experiments of **3** and **6** using $NOBF_4$. As expected, in both cases [Ru^{III}(CO)(pyS_4)]BF_4 (**17**) and [Ru^{III}(NH_3)(pyS_4)]BF_4 (**18**) formed; these complexes could be isolated and characterized. These results indicate the facility of the oxidation of the Ru center in the [Ru(pyS_4)] fragment when using oxidants such as [$FeCp_2$]PF_6, I_2, and $NOBF_4$. In the case of $NOBF_4$, the oxidation takes place without decoordination of the NH_3 and CO ligands. The formation of stable ammonia complexes, **15** and **16**, from the hydrazine complex **5** is in agreement with the observed decomposition of the hydrazine ligand in **5** to ammonia, and other compounds, mentioned above. A possible explanation for the oxidation

of **5** to **15** and **16** might be the decomposition of hydrazine to ammonia in the first step and then oxidation of Ru^{II} to Ru^{III} in the resulting ammonia complex — an intermediate species — in the second. The oxidation of **5** and **6** with H_2O_2 leads to oxidation of the thiolate donors. When H_2O_2 is added to a solution of **5** in THF, the initial red color turns to yellow and the formation of a mixture of $[\{Ru(pyS_4-O_3)\}_2]$ (**19**) and $[\{Ru(pyS_4-O_4)\}_2]$ (**20**) is observed. This yellow solid exhibits two new IR bands at 1141 and 1042 cm^{-1} that indicate the oxidation of thiolato sulfur to sulfenato/sulfinato (**19**) and sulfinato groups (**20**).[14] Several examples of the oxidation of thiolate donors in transition metal complexes appear in the literature. Although thiolates are normally oxidized to disulfides, it is known that metal-bound thiolates can be oxidized to sulfinates and sulfenates.[15,16] The X-ray crystallographic structural determination of **19** confirms the formation of dinuclear Ru^{II} species, wherein two $[Ru(pyS_4-O_3)]$ fragments are bridged by the S atom of a sulfenato group. In the case of **20**, two $[Ru(pyS_4-O_3)]$ fragments are bridged by two O atoms. Treatment of **6** with H_2O_2 led also, as in the case of **5**, to the oxidation of the thiolate donors. The elemental analysis of the isolated product was in agreement with the formation of mononuclear $[Ru(NH_3)(pyS_4-O_4)]$ (**21**). The ammonia ligand did not decoordinate during this reaction; this result is in line with our observations, discussed above, on the different stabilities of the ammonia and hydrazine ligands in the $[Ru(pyS_4)]$ fragment.

The various results of the chemical oxidation experiments of the $[Ru(pyS_4)]$ fragment prompted us to undertake electrochemical investigations using the Ru^{II} complexes **2**, **3**, **5**, **6**, **7**, and **8** and the Ru^{III} complexes **15** and **17**. The results support the hypothesis that the metal center is easy oxidized in the $[Ru(pyS_4)]$ fragment. The Ru^{II} CO complex **3** displays one quasireversible redox wave at 0.58 V, which we assign to the redox couple $[Ru(CO)(pyS_4)]^{+/2+}$. The possible chemical oxidation of thiolate donors, which we commented on above, is now corroborated by the results of the electrochemical investigations. $[Ru(NH_3)(pyS_4)]$ (**6**) exhibits an irreversible wave at 0.88 V, which we ascribe to the oxidation of thiolate donors in the pyS_4 ligand. A similar wave at 0.8 V appears in the cyclic voltammogram of the Ru^{III} ammonia complex **15**. The second reversible wave observed for **15** at 0.32 V is assigned to the $[Ru(NH_3)(pyS_4)]^{+/2+}$ redox couple. The cyclic voltammogram of **15** also exhibits one reversible wave in the cathodic region (−0.24 V); it is compatible with the reversible reduction of **15** to the Ru^{II} ammonia complex and can be assigned to the redox couple $[Ru(NH_3)(pyS_4)]^{+/0}$. The cyclic voltammograms of **2**, **7**, and **8** exhibit reversible redox waves in the anodic region that are typical of $[Ru(L)(pyS_4)]$ (L = MeCN, py, pyr): at 0.07, 0.06, and 0.12 V, respectively. In the case of **2**, we also observed a reversible redox wave in the cathodic region at −0.2 V, which we assign to the redox couple $[Ru(NCMe)(pyS_4)]^{0/-1}$. The difficulties in oxidizing the hydrazine complex **5** to a diazene complex are in good agreement with the electrochemical properties of **5**. No redox waves were observable in the anodic region of the voltammogram of **5**. One quasireversible redox wave at −0.13 V is assigned to the redox couple Ru^{II}/Ru^{I}.

Characterization of $[Ru(L)(pyS_4)]$ Complexes

As far as possible, we characterized all of the complexes by elemental analyses and IR, NMR, and mass spectra. The molecular structures of **4**, **6**, **10**, **14**, **15**, **19**, **20**, **22**, **23**, and **24** were determined by X-ray crystallographic analyses. The Ru^{II} complexes (including **6** and **7**) are soluble in CH_2Cl_2, THF, DMF, and DMSO, but they are insoluble in MeOH, Et_2O, and hexane. Complexes **6** and **7** are soluble in all common solvents. The Ru^{III} complexes display better solubility in MeOH and are rather sparingly soluble in CH_2Cl_2 and THF. All Ru^{II} complexes proved to be diamagnetic, while the Ru^{III} complexes are paramagnetic, as indicated by their ^1H NMR spectra. The ^1H NMR spectra of $[Ru^{II}(L)(pyS_4)]$ complexes exhibit a typical set of four or five multiplets for the 11 aromatic protons ($\delta \approx 9-6$ ppm) and two typical patterns for an AB spin system representing the diastereotopic methylene protons ($\delta \approx 5.5-4.5$ ppm). In the case of **20**, all of the pairs of methylene protons of the oxidized pyS_4 ligand are diastereotopic because of the stereogenic center at the S atom of the bridging sulfinic group. Typically, we observed a characteristic triplet that is due to the pyridine H_γ protons. The ^1H NMR spectra of **2**, **6**, and **21** exhibit characteristic singlets at $\delta = 2.16$, 1.54, and 1.52 ppm, respectively, that indicate the coordination of acetonitrile and ammonia ligands. The hydrazine complex **5** gave rise to two singlets at $\delta = 4.86$ and 4.01 ppm, which we assign to the Ru-bound NH_2 group and terminal NH_2 group. In the $^{13}C\{^1H\}$ NMR spectra, the 17 aromatic and 2 aliphatic carbon atoms of the $[Ru(pyS_4)]$ fragments resulted in 10 signals (9 and 1, respectively). The electronic absorption spectra of **5** and **6** in DMF each consist of two strong bands with maxima at 347 and 504 nm; **7** and **8** exhibit absorptions at ca. 400 and 509 nm (for **7**) and 557 nm (for **8**). Absorption at > 500 nm arises from thiolate-to-ruthenium(II) charge-transfer transitions. The blue shift of the pyrazine complex **8** is compatible with its deep violet color compared to the red pyridine complex **7**. The presence of the pyridine unit in the pyS_4 ligand is associated with an absorption at ca. 400 nm. Complex **15** displays absorptions at 596 and 822 nm.

X-ray Structural Analyses

X-ray structural analyses corroborated the spectroscopic results for several of the complexes. Figure 1−3 depict the molecular structures of $[\{Ru(pyS_4)\}_2]\cdot 2$toluene (**4**·2-toluene), $[Ru(NH_3)(pyS_4)]$(**6**), $[Ru(I)(pyS_4)]\cdot 1.5CH_2Cl_2$ (**10**·$1.5CH_2Cl_2$), $[\{Ru(pyS_4)\}_2](PF_6)\cdot CD_2Cl_2$ (**14**·CD_2Cl_2), $[Ru(NH_3)(pyS_4)]PF_6\cdot CH_2Cl_2$ (**15**·CH_2Cl_2), and $0.68[\{Ru(pyS_4-O_3)\}_2]\cdot 0.32[\{Ru(pyS_4-O_4)\}_2]\cdot 2MeOH$ (0.68 **19**·0.32 **20**·2MeOH). We also report the structures of $[\{Ru(pyS_4)\}_2](I_3)_2\cdot 1.8THF$ (**22**·1.8THF), $[\{Ru(pyS_4\text{-}Et)\}_2](BF_4)_2(B_2F_7)\cdot 3CD_2Cl_2$ (**23**·$3CD_2Cl_2$), and $[\{Ru(pyS_4)\}_2](BF_4)(B_2F_7)\cdot 3CH_2Cl_2$ (**24**·$3CH_2Cl_2$), which we only characterized by X-ray crystallography.

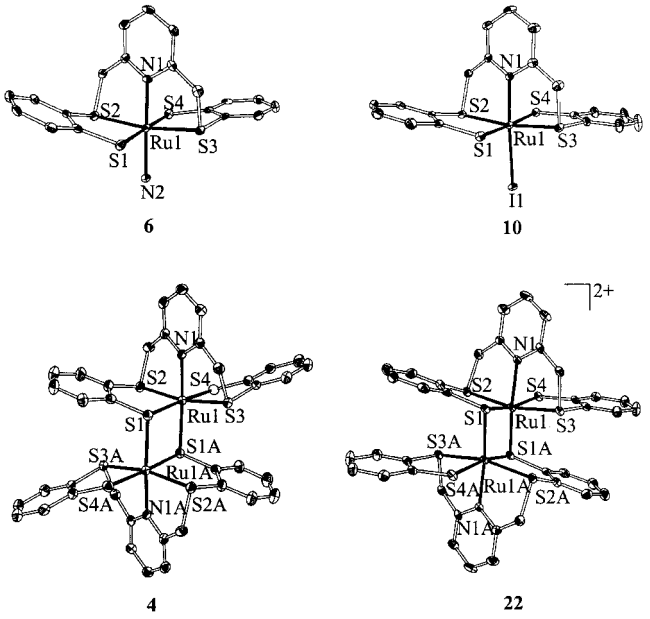

Figure 1. Molecular structures of [{Ru(pyS$_4$)}$_2$]·2 toluene (**4**·2toluene), [Ru(NH$_3$)(pyS$_4$)] (**6**), [Ru(I)(pyS$_4$)]·1.5 CH_2Cl_2 (**10**·1.5CH_2Cl_2), and [{Ru(pyS$_4$)}$_2$](I$_3$)$_2$·1.8THF (**22**·1.8THF); 50% probability ellipsoids, H atoms, solvent molecules, and I_3^- anions omitted

Table 1−3 list selected distances and angles of these complexes.

In all of the complexes, the ruthenium centers exhibit pseudo-octahedral coordination. Thiolate and thioether donors always adopt *trans* positions in the [RuS$_4$] cores. This observation proves the steric rigidity of the py(CH$_2$)$_2$ backbone. In the mononuclear complexes **6**, **10**, and **15**, the Ru centers are coordinated by one N and four S donors of the pentadentate pyS_4^{2-} ligand and a sixth ligand (NH$_3$ or I), while in the dinuclear complexes **4**, **14**, **19**, **20**, **22**, **23**, and **24** the sixth ligand is a thiolate donor of the second [Ru(pyS$_4$)] unit. In mono- and dinuclear Ru^{II} complexes, the Ru−S (thiolate) distances are slightly longer than the Ru−S (thioether) distances, but all the Ru−S distances in the Ru^{III} complexes are of similar length. The Ru−N (pyridine) distances in all the Ru^{II} complexes are slightly shorter (by ca. 4 pm) than in the Ru^{III} complexes.

In the case of **19** and **20**, two different orientations were refined for the oxygen atoms, with an occupancy of 68% for O1, O3, and O4 and 32% for O1′, O2′, O3, and O4. The ethyl groups in **23** are situated at the S atoms S4 and S4A that are *trans* to the bridging S donors S1 and S1A, respectively. The dimer **4** that has two Ru^{II} centers possesses crystallographically imposed C_i symmetry. The mixed-valence complex **14** exhibits approximate C_2 symmetry. The two

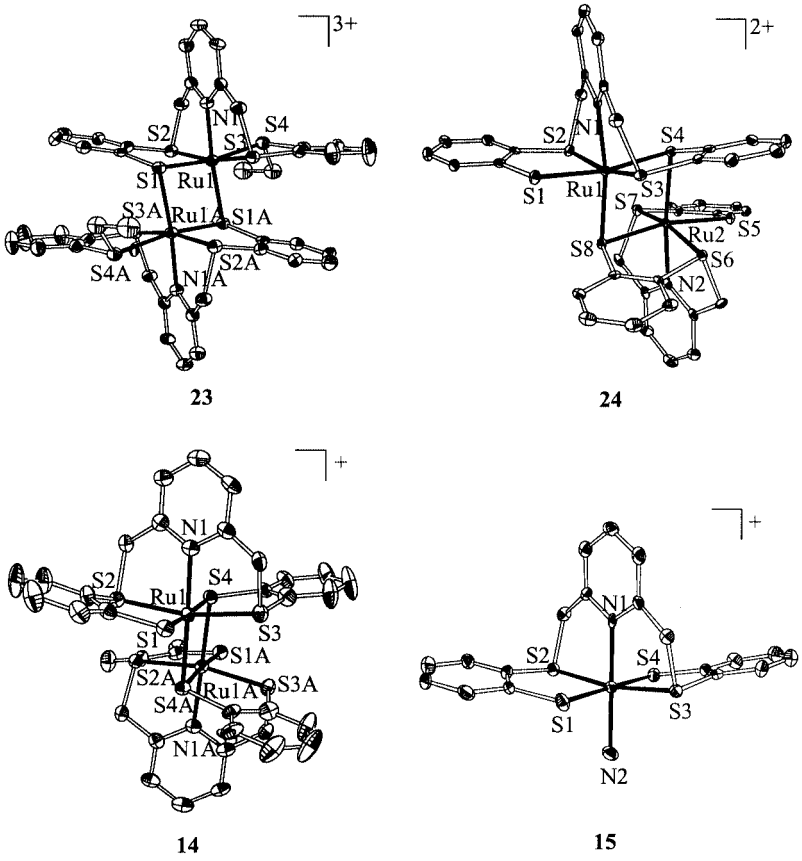

Figure 2. Molecular structures of [{Ru(pyS$_4$)}$_2$](PF$_6$)·CD_2Cl_2 (**14**·CD_2Cl_2), [Ru(NH$_3$)(pyS$_4$)]PF_6·CH_2Cl_2 (**15**·CH_2Cl_2), [{Ru(pyS$_4$-Et)}$_2$](BF$_4$)$_2$(B$_2$F$_7$)·3CD_2Cl_2 (**23**·3CD_2Cl_2), and [{Ru(pyS$_4$)}$_2$](BF$_4$)(B$_2$F$_7$)·3CH_2Cl_2 (**24**·3CH_2Cl_2); 50% probability ellipsoids, H atoms, solvent molecules, and BF_4^-, $B_2F_7^-$, and PF_6^- anions omitted

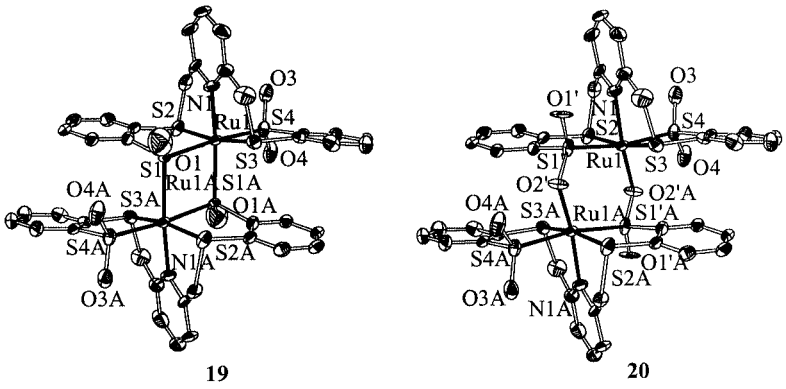

Figure 3. Molecular structures of $[\{Ru(pyS_4-O_3)\}_2]$/$[\{Ru(pyS_4-O_4)\}_2]$·2MeOH (**19**/**20**·2MeOH); 50% probability ellipsoids, H atoms, and solvent molecules omitted

Table 1. Selected distances (pm) and angles (°) in $[Ru(NH_3)(pyS_4)]$ (**6**), $[Ru(I)(pyS_4)]$·$1.5CH_2Cl_2$ (**10**·$1.5CH_2Cl_2$), and $[Ru(NH_3)(pyS_4)]$-PF_6·CH_2Cl_2 (**15**·CH_2Cl_2)

Compound	**6**	**10**·$1.5CH_2Cl_2$	**15**·CH_2Cl_2
Ru1−N1	202.3(3)	207.7(3)	206.7(5)
Ru1−S1	237.7(1)	230.3(1)	232.6(2)
Ru1−S2	231.3(1)	232.9(1)	233.0(2)
Ru1−S3	229.8(1)	231.0(1)	232.2(2)
Ru1−S4	238.7(1)	234.1(1)	229.7(2)
Ru1−L	214.2(3)	271.24(4)	213.2(5)
S1−Ru1−S2	87.08(3)	88.27(4)	88.22(7)
S2−Ru1−S4	93.90(3)	92.71(3)	92.27(7)
S4−Ru1−S3	87.56(3)	88.55(3)	88.76(7)
S1−Ru1−S3	91.65(3)	89.74(4)	90.98(7)
N1−Ru1−S2	84.11(9)	84.38(9)	84.1(2)
N1−Ru1−S1	91.79(9)	89.78(8)	90.7(2)
N1−Ru1−L	178.5(2)	176.51(8)	179.9(3)

Table 2. Selected distances (pm) and angles (°) in $[\{Ru(pyS_4)\}_2]$·2toluene (**4**·2toluene), $[\{Ru(pyS_4-O_3)\}_2]$/$[\{Ru(pyS_4-O_4)\}_2]$·2MeOH (**19**/**20**·2MeOH), and $[\{Ru(pyS_4)\}_2]$-$(I_3)_2$·1.8THF (**22**·1.8THF)

Compound	**4**·2toluene	**19**/**20**·2MeOH	**22**·1.8THF
Ru1−N1	205.3(4)	205.9(5)	210.4(4)
Ru1−S1	237.1(2)	236.2(4)	230.6(2)
Ru1−S2	231.2(2)	231.7(2)	235.9(2)
Ru1−S3	230.6(2)	230.6(2)	234.3(2)
Ru1−S4	238.4(2)	230.4(2)	239.2(2)
Ru1−S1A	240.9(2)	238.4(6)	231.0(2)
S1−O1	–	140.0(2)	–
S4−O3	–	149.3(5)	–
S1−Ru1−S2	87.46(5)	87.5(1)	88.57(5)
S2−Ru1−S4	92.63(5)	94.18(6)	91.65(4)
S4−Ru1−S3	87.18(5)	88.28(6)	87.86(4)
S1−Ru1−S3	93.50(5)	91.1(2)	89.24(4)
N1−Ru1−S2	83.4(2)	84.5(2)	82.6(2)
N1−Ru1−S1	91.7(2)	95.8(2)	86.8(2)
S1−Ru1−S1A	83.80(5)	76.3(2)	105.46(4)
Ru1−S1−Ru1A	96.20(5)	103.7(2)	74.54(4)
O4−S4−O3	–	111.0(3)	–
O1−S1−Ru1A	–	119.6(6)	–

Table 3. Selected distances (pm) and angles (°) in $[\{Ru(pyS_4)\}_2](PF_6)$·CD_2Cl_2 (**14**·CD_2Cl_2), $[\{Ru(pyS_4\text{-}Et)\}_2]$-$(BF_4)_2(B_2F_7)$·$3CD_2Cl_2$ (**23**·$3CD_2Cl_2$), and $[\{Ru(pyS_4)\}_2](BF_4)$-(B_2F_7)·$3CH_2Cl_2$ (**24**·$3CH_2Cl_2$)

Compound	**14**·CD_2Cl_2	**23**·$3CD_2Cl_2$	**24**·$3CH_2Cl_2$
Ru−N1	210.4(6)	208.2(5)	215.5(3)
Ru1−S1	236.4(2)	233.3(2)	239.0(2)
Ru1−S2	232.5(2)	234.4(2)	234.2(2)
Ru1−S3	231.7(2)	231.3(2)	235.4(2)
Ru1−S4	236.6(2)	237.6(2)	233.4(2)
Ru1−S1A	236.4(2)[a]	236.3(2)	234.4(2)[b]
S1−Ru1−S2	88.17(8)	88.10(6)	87.14(4)
S2−Ru1−S4	92.92(8)	93.34(6)	93.83(4)
S4−Ru1−S3	88.36(8)	87.31(6)	87.93(4)
S1−Ru1−S3	89.43(8)	89.14(6)	88.39(4)
N1−Ru1−S2	82.90(2)	83.6(2)	83.0(1)
N1−Ru1−S1	89.8(2)	87.8(2)	82.20(9)
S1−Ru1−S1A	89.16(7)	98.52(5)	88.44(4)[b]
Ru1−S1−Ru1A	84.40(6)	81.48(5)	77.46(3)[c]

[a] S1A = S4A. [b] S1A = S8. [c] S1 = S8, Ru1A = Ru2.

Ru^{III} fragments in dimeric **22** are connected by a crystallographic inversion center. The dinuclear complex **23** contains one *R* and one *S* [Ru(pyS$_4$-Et)] enantiomer, while in the mixed-valence complex **24** always two identical enantiomers [(*R*,*R*) or (*S*,*S*)] occurred.

Conclusion

The aim of this work was the synthesis of new labile $[Ru(L)(pyS_4)]$ complexes. We have found that $[Ru(MeCN)(pyS_4)]$ (**2**) is a good precursor for other complexes. This complex allows the synthesis of $[Ru(CO)(pyS_4)]$ (**3**), $[Ru(N_2H_4)(pyS_4)]$ (**5**), and $[Ru(NH_3)(pyS_4)]$ (**6**), which contain nitrogenase-relevant ligands. The $[Ru(pyS_4)]$ fragment can bind a further σ ligand, such as N_3^-, in contrasting to the $[Fe(pyS_4)]$ fragment, which does not coordinate NH_3 and N_3^- ligands. Moreover, the coordination of the nitrogenase-relevant molecules takes place under rather mild conditions. The replacement of the flexible NH(dialkyl)

bridge of the former NHS_4^{2-} ligand with the sterically more rigid dialkyl methyl pyridine bridge in the pyS_4^{2-} ligand successfully enforces a *trans*-thiolate configuration in [Ru(L)(pyS_4)] complexes. The synthesis of complexes such as [Ru^{III}(NH_3)(pyS_4)]X (X = PF_6, I, BF_4) (**15**, **16**, **18**) and [Ru^{III}(CO)(pyS_4)]BF_4 (**17**) proves that the oxidation of Ru^{II} to Ru^{III} centers occurs readily in the [Ru(pyS_4)] fragment. Interestingly, both [Ru(N_2H_4)(pyS_4)] (**5**) and [Ru(NH_3)(pyS_4)] (**6**) can be converted readily into the corresponding sulfinato species upon reaction with H_2O_2. We have proven the different lability of hydrazine and ammonia ligands in [Ru(pyS_4)] fragments by studying their reactivity towards a range of oxidants.

Experimental Section

General Methods: Unless noted otherwise, all reactions and operations were carried out under nitrogen and at room temp. using standard Schlenk techniques and absolute solvents. As far as possible, reactions were monitored by IR and NMR spectroscopy. Spectra were recorded using the following instruments: IR (KBr disks or CaF_2 cuvettes, solvent bands were compensated): Perkin−Elmer 16 PC FT IR. NMR: JEOL FT-JNM-GX 270, EX 270, and Lambda LA 400; spectra are referenced to residual protiosolvent signals; chemical shifts are quoted on the δ scale (downfield shifts are positive) relative to tetramethylsilane (^{1}H, ^{13}C{^{1}H} NMR); spectra were recorded at 25 °C. Mass spectra: JEOL JMS 700 spectrometer. UV-Vis-NIR: Varian Cary 50, quartz cuvettes (hellma, d = 1 cm). Elemental Analysis: Carlo−Erba EA 1106 and 1108 analyzer. Cyclic voltammetry was performed with a PAR 264A potentiostat using a three-electrode cell with glassy carbon ROTEL A working, Pt reference, and Pt counter electrodes. The concentration of each complex was 10^{-3} M. NBu_4PF_6 (10^{-1} M) was used as the conducting electrolyte. Potentials are referenced to the NHE via Fc/Fc^+ as internal standard (E = +0.41 V vs. NHE).[17] Reagents (N_2H_4·H_2O, pyridine, pyrazine, LiOMe, Et_3OBF_4, HBF_4/Et_2O, $NOBF_4$, and H_2O_2) were purchased from Merck, Fluka, Aldrich, and Acros. [Ru(NO)(pyS_4)]Br (**1**) was prepared as described in the literature.[7b]

[Ru(NCMe)(pyS_4)] (2): N_2H_4·H_2O (0.034 mL, 0.704 mmol) was added to a brown-violet suspension of **1** (210 mg, 0.352 mmol) in MeCN (20 mL). The color of the suspension turned to carrot-orange. The suspension was stirred for 2 h, during the course of which time an orange solid formed; this solid was filtered, washed with MeOH (2 × 20 mL) and Et_2O (20 mL), and dried in vacuo. Yield: 155 mg of **2** (80%). $C_{21}H_{18}N_2RuS_4$ (527.67): calcd. C 47.80, H 3.43, N 5.31, S 24.31; found C 47.35, H 3.59, N 5.87, S 23.30. IR (KBr): $\tilde{\nu}$ = 2262 cm^{-1} (ν_{CN}). ^{1}H NMR (269.6 MHz, CD_2Cl_2/CD_3CN): δ = 7.63−7.56 (m, 2 H, C_6H_4), 7.41−7.35 (m, 2 H, C_6H_4), 7.11 (t, 1 H, C_5H_3N), 6.93 (d, 2 H, C_5H_3N), 6.88−6.77 (m, 4 H, C_6H_4), 4.64 (d, $^3J_{H,H}$ = 17.8 Hz, 2 H, CH_2), 4.44 (d, $^3J_{H,H}$ = 17.8 Hz, 2 H, CH_2), 2.16 (s, 3 H, CH_3) ppm. ^{13}C{^{1}H} NMR (67.7 MHz, CD_2Cl_2): δ = 158.7, 157.1, 132.2, 131.8, 131.2, 130.2, 127.4, 120.6, 120.1 (C_6H_4), 116.5 (MeCN), 55.6(CH_2) ppm.

[Ru(CO)(pyS_4)] (3): CO gas was bubbled through a red-orange suspension of **2** (200 mg, 0.38 mmol) in THF (20 mL). Instantly, the color of the suspension changed to yellow. After stirring for 24 h under an atmosphere of CO, the resulting yellow suspension was filtered. The filtrate was evaporated to dryness and the resulting yellow powder was washed with MeOH (20 mL) and dried in vacuo. Yield: 178.2 mg of **3**·MeOH (86%). $C_{21}H_{19}NO_2RuS_4$ (546.70): calcd. C 46.14, H 3.50, N 2.56, S 23.46, found C 45.84, H 3.84, N 2.45, S 23.10. IR (KBr): $\tilde{\nu}$ = 1959.4 cm^{-1} (ν_{CO}). ^{1}H NMR (269.6 MHz, CD_2Cl_2): δ = 7.67−7.62 (m, 2 H, C_6H_4), 7.49−7.42, (m, 4 H, C_6H_4), 7.23 (d, $J_{H,H}$ = 13.5 Hz, 2 H, C_5H_3N), 7.03−6.95 (m, 4 H, C_6H_4/C_5H_3N), 5.12 (d, 2 H, CH_2), 5.07 (d, 2 H, CH_2) ppm. ^{13}C{^{1}H} NMR (67.7 MHz, CD_2Cl_2): δ = 201.7 (CO), 156.3, 155.9, 136.8, 132.5, 131.1, 131.0, 129.16, 122.6, 122.0 (C_6H_4) 58.2 (CH_2) ppm. MS (FD, CH_2Cl_2, ^{102}Ru): m/z = 515 [Ru(CO)(pyS_4)]$^+$.

[{Ru(pyS_4)}$_2$] (4): An orange suspension of **2** (250 mg, 0.47 mmol) in THF (30 mL) was heated under reflux for 4 days to give a red-brown suspension. The solid was filtered, washed with Et_2O (2 × 10 mL), and dried in vacuo. Yield: 156 mg of **4** (68%). $C_{38}H_{30}N_2Ru_2S_8$ (973.34): calcd. C 46.89, H 3.11, N 2.88, S 26.36; found C 45.38, H 2.76, N 2.91, S 25.44. MS (FD, DMSO, ^{102}Ru): m/z = 973 [{Ru(pyS_4)}$_2$]$^+$.

[Ru(N_2H_4)(pyS_4)] (5): An excess of N_2H_4·H_2O (0.55 mL, 11.4 mmol) was added to a suspension of **2** (300 mg, 0.57 mmol) in THF (30 mL). After 15 h, the red precipitate was separated, washed with MeOH (3 × 30 mL), and dried in vacuo. Yield: 295 mg of **5** (83%). $C_{19}H_{19}N_3RuS_4$ (518.69): calcd. C 44.00, H 3.69, N 8.10, S 24.72; found C 44.19, H 3.29, N 7.34, S 24.64. IR (KBr): $\tilde{\nu}$ = 3335, 3207, 3102 cm^{-1} (ν_{NH}). ^{1}H NMR (269.6 MHz, [D$_7$]DMF): δ = 7.75−7.72 (m, 2 H, C_6H_4), 7.45−7.42 (m, 2 H, C_6H_4), 7.12−7.06 (t, 3 H, C_5H_3N), 6.91−6.81 (m, 4 H, C_6H_4), 4.86 (s, 2 H, −N*H*$_2$−NH$_2$), 4.72 (d, $^3J_{H,H}$ = 16.2 Hz, 2 H, CH_2), 4.52 (d, $^3J_{H,H}$ = 16.2 Hz, 2 H, CH_2), 4.01 (s, 2 H, −NH$_2$−N*H*$_2$) ppm. ^{13}C{^{1}H} NMR (67.7 MHz, CD_2Cl_2): δ = 159.1, 156.7, 132.5, 132.2, 131.5, 131.2, 128.1, 121.6, 120.5 (C_6H_4), 54.6 (CH_2) ppm. MS (FD, DMF, ^{102}Ru): m/z = 973 [{Ru(pyS_4)}$_2$]$^+$.

[Ru(NH_3)(pyS_4)] (6): NH_3 was bubbled through a suspension of **2** (600 mg, 1.14 mmol) in THF (100 mL) for 15 min. The resulting red suspension was stirred under an NH_3 gas for additional 2 h and then filtered. Addition of *n*-hexane (100 mL) to the red filtrate precipitated a red powder, which was separated, washed with *n*-hexane (3 × 20 mL), and dried in vacuo. Yield: 493 mg of **6** (86%). $C_{19}H_{18}N_2RuS_4$ (503.68): calcd. C 45.31, H 3.60, N 5.56, S 25.46; found C 45.43, H 3.55, N 5.14, S 24.49. IR (KBr): $\tilde{\nu}$ = 3362, 3242, 3161 cm^{-1} (ν_{NH}). ^{1}H NMR (269.6 MHz, CD_2Cl_2): δ = 7.67−7.64 (m, 2 H, C_6H_4), 7.52−7.46 (m, 2 H, C_6H_4), 7.10−7.06 (t, 3 H, C_5H_3N), 6.93−6.88 (m, 4 H, C_6H_4), 4.65 (d, $^3J_{H,H}$ = 16.2 Hz, 2 H, CH_2), 4.46 (d, $^3J_{H,H}$ = 16.2 Hz, 2 H, CH_2), 1.54 (s, 3 H, −NH_3) ppm. MS (FD, CH_2Cl_2, ^{102}Ru): m/z = 973 [{Ru(pyS_4)}$_2$]$^+$, 504 [Ru(NH_3)(pyS_4)]$^+$.

[Ru(py)(pyS_4)] (7): A suspension of **2** (340 mg, 0.64 mmol) in pyridine (25 mL) was heated under reflux for 5 min. The resulting red solution was evaporated to yield a red solid. Yield: 340 mg of **7**·py (82.38%). $C_{29}H_{25}N_3RuS_4$ (644.85): calcd. C 54.02, H 3.91, N 6.52, S 19.89; found C 54.04, H 4.51, N 6.50, S 20.19. ^{1}H NMR (269.6 MHz, CD_2Cl_2): δ = 8.58 (d, $J_{H,H}$ = 5.4 Hz, 2 H, C_5H_5N) 8.41−8.38 (m, 2 H, C_6H_4), 7.69−7.65 (m, 2 H, C_6H_4), 7.52 (d, $J_{H,H}$ = 8.1 Hz, 2 H, C_5H_3N), 7.46−7.40 (t, 1 H, C_5H_5N), 7.31−7.26 (m, 2 H, C_5H_5N), 7.10−7.04 (t, 1 H, C_5H_3N), 6.95−6.89 (m, 4 H, C_6H_4), 4.77 (d, $^3J_{H,H}$ = 16.2 Hz, 2 H, CH_2), 4.47 (d, $^3J_{H,H}$ = 16.2 Hz, 2 H, CH_2) ppm. ^{13}C{^{1}H} NMR (67.7 MHz, CD_2Cl_2): δ = 159.38, 156.74, 150.05, 136.01, 134.82, 132.54, 132.24, 131.55, 128.10, 123.91, 123.77, 120.62 (C_6H_4), 56.5 (CH_2) ppm. MS (FD, CH_2Cl_2, ^{102}Ru): m/z = 973 [{Ru(pyS_4)}$_2$]$^+$.

[Ru(pyrazine)(pyS_4)] (8): An excess of pyrazine (4.0 g, 49 mmol) was added to a suspension of **2** (340 mg, 0.64 mmol) in THF (40 mL).

The reaction mixture was heated under reflux for 15 min. The resulting deep-violet solution was evaporated to yield a violet powder, which was washed with *n*-hexane (5 × 30 mL) and dried in vacuo. Yield: 210 mg of **8**·0.25 pyrazine (54.22%). $C_{29}H_{25}N_3RuS_4$ (586.78): calcd. C 49.13, H 3.44, N 7.75, S 21.86; found C 48.09, H 3.60, N 7.86, S 20.76. ^{1}H NMR (269.6 MHz, CD_2Cl_2): δ = 8.56 (s, free pyrazine), 8.38 (d, $J_{H,H}$ = 5.4 Hz, 2 H, C_4H_4), 8.07 (d, $J_{H,H}$ = 5.4 Hz, 2 H, C_4H_4), 7.69 (d, $J_{H,H}$ = 16.2 Hz, 2 H, C_6H_4) 7.52 (d, $J_{H,H}$ = 10.8 Hz, 2 H, C_5H_3N), 7.21−7.15 (t, 1 H, C_5H_3N), 6.99−6.88 (m, 6 H, C_6H_4), 4.80 (d, $^3J_{H,H}$ = 16.2 Hz, 2 H, CH_2), 4.50 (d, $^3J_{H,H}$ = 13.5 Hz, 2 H, CH_2) ppm. $^{13}C\{^1H\}$ NMR (67.7 MHz, CD_2Cl_2): δ = 159.14, 156.94, 152.20, 145.40 (free pyrazine), 144.05, 133.14, 132.63, 131.12, 131.00, 121.81, 120.93 (C_6H_4), 56.46 (CH_2) ppm. MS (FD, CH_2Cl_2, ^{102}Ru): *m*/*z* = 973 $[\{Ru(pyS_4)\}_2]^+$, 567 $[Ru(pyr)(pyS_4)]^+$.

[Ru(I)(pyS$_4$)] (10): I_2 (0.27 g, 1.08 mmol) was added to a suspension of **2** (1.15 g, 2.16 mmol) in THF (50 mL). The resulting violet suspension was stirred for 30 min and then filtered. *n*-Hexane (100 mL) was added to the filtrate. After 30 min, the violet precipitate was filtered, washed with *n*-hexane (2 × 20 mL) and Et_2O (2 × 20 mL), and dried in vacuo for 1 h. Yield: 0.65 g of **10** (48.9%). $C_{19}H_{15}NRuS_4I$ (613.55). MS (FD, THF, ^{102}Ru): *m*/*z* = 614 $[Ru(I)(pyS_4)]^+$, 973 $[\{Ru(pyS_4)\}_2]^+$.

[Ru(NCMe)(pyS$_4$-H)]BF$_4$ (11): HBF_4 (0.11 mL, 54% solution in Et_2O, 0.77 mmol) was added to a suspension of **2** (406 mg, 0.77 mmol) in CH_2Cl_2 (20 mL) at −78 °C. The color of the suspension changed to yellow-green. The reaction mixture was stirred for 2 h at −78 °C and then filtered. *n*-Hexane (50 mL) was added to the green filtrate. The green precipitate was separated by filtration and dried in vacuo for 15 min. IR (KBr): $\tilde{\nu}$ = 2472 (ν_{SH}), 2273 (ν_{CN}), 1055 (ν_{BF}) cm^{-1}. MS (FD, DMF, ^{102}Ru): *m*/*z* = 976 $[\{Ru(pyS_4\text{-}H)\}_2]^+$.

[Ru(NCMe)(pyS$_4$-Et)]BF$_4$ (12): Et_3OBF_4 (1.19 mL, 1 M solution in CH_2Cl_2, 1.19 mmol) was added to a suspension of **2** (627 mg, 1.19 mmol) in CH_2Cl_2 (30 mL). The color changed to yellow-brown and, after 2 h, the brown solid was separated by filtration. *n*-Hexane (70 mL) was added to the deep yellow-brown filtrate. The yellow precipitate was filtered, washed with *n*-hexane (20 mL), and dried in vacuo. $C_{23}H_{23}N_2RuS_4BF_4$ (643.56). IR (KBr): $\tilde{\nu}$ = 2282 (ν_{CN}), 1048 (ν_{BF}) cm^{-1}. ^{1}H NMR (269.6 MHz, CD_2Cl_2): δ = 8.25 (d, $J_{H,H}$ = 5.4 Hz, 2 H, C_5H_3N), 7.77−6.93 (m, 9 H, aryl), 5.00, 4.85, 4.73, 4.55 (4 × d, 8 H, CH_2), 3.18 (m, 2 H, CH_2), 2.39 (s, 3 H, coord. CH_3CN), 2.23 (s, 3 H, free CH_3CN), 1.50 (t, 3 H, CH_3) ppm. $^{13}C\{^1H\}$ NMR (67.7 MHz, CD_2Cl_2): δ = 159.2, 155.0, 138.15, 135.6, 134.8, 133.7, 133.5, 133.3, 133.0, 132.9, 132.4, 131.9, 131.6, 130.4, 122.9, 122.3 (C_6H_5), 123.9 (CH_3CN), 55.7 (CH_2), 55.5 (CH_2), 38.1 (CH_2), 13.0 (CH_3), 4.6 (CH_3CN) ppm. MS (FD, CH_2Cl_2, ^{102}Ru): *m*/*z* = 516 $[Ru(pyS_4\text{-}Et)]^+$.

[{Ru(pyS$_4$-Et)}$_2$](BF$_4$)$_2$ (13): Et_3OBF_4 (5.16 mL, 1 M solution in CH_2Cl_2, 6.35 mmol) was added to a suspension of **2** (670 mg, 1.27 mmol) in CH_2Cl_2 (30 mL) and then the mixture was stirred for 2 days. During this period of time, the mixture became a yellow-green solution. Upon addition of Et_2O (20 mL) and THF (30 mL), a yellow solid precipitated; it was filtered and dried in vacuo. $C_{42}H_{40}N_2Ru_2S_8B_2F_8$ (1205.02). IR (KBr): $\tilde{\nu}$ = 1060 cm^{-1} (ν_{BF}). ^{1}H NMR (399.65 MHz, CD_2Cl_2): δ = 8.23 (d, $J_{H,H}$ = 8.1 Hz, 2 H), 7.78−7.25 (m, 9 H, C_6H_5), 5.01 (d, $^3J_{H,H}$ = 24.0 Hz, 2 H, CH_2), 4.84 (d, $^3J_{H,H}$ = 28.0 Hz, 2 H, CH_2), 3.24 (m, 4 H, CH), 2.39 (s, 3 H, free CH_3CN), 1.53 (t, 6 H, CH_3) ppm. $^{13}C\{^1H\}$ NMR (67.7 MHz, CD_2Cl_2): δ = 159.4, 138.3, 134.9, 134.5, 133.4, 133.2, 133.1, 132.5, 130.5 [C_6H_5], 124.0 (free CH_3CN), 55.2 (CH_2), 38.1 (CH_2), 13.0 (CH_3), 4.5 (free CH_3CN) ppm. MS (FD, CH_2Cl_2, ^{102}Ru): *m*/*z* = 585 $[Ru(pyS_4-Et_2)(MeCN)]^{2+}$, 1033 $[\{Ru(pyS_4-Et_2)\}_2]^+$.

[{Ru$^{II/III}$(pyS$_4$)}$_2$](PF$_6$) (14): LiOMe (0.77 mL, 1 M MeOH solution) and $[FeCp_2]PF_6$ (255 mg, 0.77 mmol) were added sequentially to a red solution of **5** (200 mg, 0.386 mmol) in DMF (20 mL) and then the mixture was stirred overnight. During this period of time, red microcrystals formed; they were isolated by filtration and identified as dimeric **4** (ca. 25 mg). Crystals grew from the deep-red filtrate; they were identified by an X-ray structural analysis to be **14**·CD_2Cl_2.

[Ru(NH$_3$)(pyS$_4$)](PF$_6$) (15). From 6: $[FeCp_2]PF_6$ (a small spatula's worth) was added to a red suspension of **6** (80 mg, 0.16 mmol) in THF (10 mL). The resulting green suspension was filtered and Et_2O (30 mL) was added to the green filtrate. The green precipitate was filtered, washed with Et_2O (2 × 10 mL), and dried in vacuo. Yield: 40 mg of **15** (32%). $C_{23}H_{26}F_6N_2OPRuS_4$ (**15**·THF) (720.75): calcd. C 38.33, H 3.89, N 3.64, S 17.79; found C 37.45, H 3.36, N 3.64, S 17.13. IR (KBr): $\tilde{\nu}$ = 3356, 3283, 3187 (ν_{NH}) cm^{-1}. MS (FD, CH_2Cl_2, ^{102}Ru): *m*/*z* = 973 $[\{Ru(pyS_4)\}_2]^+$, 504 $[Ru(NH_3)(pyS_4)]^+$.

From 5: $[FeCp_2]PF_6$ (a small spatula's worth) was added to a red suspension of **5** (230 mg, 0.44 mmol) in THF (30 mL). The resulting green suspension was filtered and then Et_2O (60 mL) was added to the green filtrate. The green precipitate was filtered, washed with Et_2O (2 × 20 mL), and dried in vacuo. Yield: 49 mg of **15** (59%).

[Ru(NH$_3$)(pyS$_4$)](I) (16): I_2 (225 mg, 0.9 mmol) was added to a red suspension of **5** (465 mg, 0.9 mmol) in THF (20 mL) and then the mixture was stirred for 30 min. The resulting yellow-brown solid was separated by filtration, washed with THF (3 × 20 mL), and dried in vacuo. Yield: 140 mg of **15** (47%). $C_{21}H_{22}IN_2O_{0.5}RuS_4$ (**16**·0.5THF) (666.64): calcd. C 37.84, H 3.33, N 4.20, S 19.24; found C 37.84, H 2.89, N 3.99, S 18.44.

[Ru(CO)(pyS$_4$)](BF$_4$) (17): $NOBF_4$ (20.54 mg, 0.17 mmol) was added at 0 °C to a yellow solution of **3** (90 mg, 0.17 mmol) in CH_2Cl_2 (30 mL). The reaction mixture was stirred at room temp. until a green solution formed (ca. 1 h); it was evaporated to yield a green solid. $C_{20.5}H_{16}BCl_2F_4NORuS_4$ (**17**·0.5CH_2Cl_2) (643.93): calcd. C 38.24, H 2.50, N 2.17, S 19.92; found C 35.93, H 2.33, N 2.40, S 18.73. IR (KBr): $\tilde{\nu}$ = 2004.5 cm^{-1}(ν_{CO}).

[Ru(NH$_3$)(pyS$_4$)](BF$_4$) (18): A red solution of **6** (325 mg, 0.65 mmol) in CH_2Cl_2 (30 mL) was combined with $NOBF_4$ (78.54 mg, 0.65 mmol) at 0 °C. The solution was stirred for 1 h at 0 °C and then for an additional 1 h at room temp. until its color had changed to green. Evaporation of the solvent gave a violet oil, which was redissolved in MeOH (30 mL). Et_2O (40 mL) was added to the resulting violet-brown solution. The green precipitate was separated and dried in vacuo. Yield: 130 mg of **18**·CH_2Cl_2 (30%). $C_{23}H_{26}F_6N_2OPRuS_4$ (675.87): calcd. C 35.54, H 2.98, N 4.15, S 18.98; found C 34.55, H 2.70, N 4.17, S 19.05.

[{Ru(pyS$_4$−O$_3$)}$_2$]/[{Ru(pyS$_4$−O$_4$)}$_2$] (19/20): H_2O_2 (1 mL) was added at room temp. to a red suspension of **5** (220 mg, 0.42 mmol) in THF (30 mL) and then the mixture was stirred for 30 min. During this period of time the color of the suspension changed to yellow. The yellow solid was separated by filtration and dried in vacuo. $C_{38}H_{30}N_2O_{8.64}Ru_2S_8$ (0.68[{Ru(pyS$_4$−O$_3$)}$_2$] × 0.32[{Ru(pyS$_4$−O$_4$)}$_2$]) (1143.65). IR (KBr): $\tilde{\nu}$ = 1141, 1042 (ν_{SO}) cm^{-1}. ^{1}H NMR (269.6 MHz, MeOD): δ = 8.09−8.00 (m, 4 H, C_6H_4 × 2),

7.84−7.77 (m, 8 H, C_6H_4), 7.59−7.47 (m, 16 H, C_6H_4), 7.35−7.23 (m, 4 H, C_5H_3N), 7.14−7.06 (m, 8 H, C_5H_3N), 5.41 (d, $J_{H,H}$ = 16.2 Hz, 2 H, CH_2), 5.40 (d, $J_{H,H}$ = 16.2 Hz, 2 H, CH_2), 4.68 (d, $J_{H,H}$ = 16.2 Hz, 2 H, CH_2), 4.67 (d, $J_{H,H}$ = 18.9 Hz, 2 H, CH_2) ppm. MS (FD, MeOH, ^{102}Ru): *m*/*z* = 1101 $[\{Ru(pyS_4{-}O_4)\}_2]^+$, 1068 $[\{Ru(pyS_4{-}O_3)\}_2]^+$, 974 $[\{Ru(pyS_4)\}_2]^+$, 486 $[Ru(pyS_4)]^+$.

[Ru(NH$_3$)(pyS$_4$−O$_4$)] (21): A red solution of **6** (205 mg, 0.41 mmol) in THF (50 mL) was combined with H_2O_2 (1 mL) at room temp. The resulting yellow precipitate was stirred for 1 h, then filtered, washed with THF (30 mL), and dried in vacuo. Yield: 201.54 mg of **21**·0.5THF (82%). $C_{21}H_{22}N_2RuS_4O_{4.5}$ (603.73): calcd. C 41.78, H 3.67, N 4.64, S 21.24; found C 38.99, H 3.55, N 4.37, S 20.81. IR (KBr): $\tilde{\nu}$ = 3353, 3301, 3188 (ν_{NH}), 1134, 1013 (ν_{SO}) cm^{-1}. ^{1}H NMR (269.6 MHz, CD_2Cl_2): δ = 7.92−7.84 (m, 4 H, C_6H_4), 7.53−7.49 (m, 4 H, C_6H_4), 7.33−7.27 (t, 3 H, C_5H_3N), 7.08 (d, $J_{H,H}$ = 8.1 Hz, 2 H, C_6H_4), 5.82 (d, $J_{H,H}$ = 16.2 Hz, 2 H, CH_2), 4.47 (d, $J_{H,H}$ = 16.2 Hz, 2 H, CH_2), 1.52 (s, 3 H, $-NH_3$) ppm. ^{13}C{^{1}H} NMR (67.7 MHz, CD_3OD): δ = 161.4, 159.7, 136.7, 133.3, 132.5, 132.2, 128.8, 123.8, 122.5 (C_6H_5), 54.9 (CH_2) ppm.

[{Ru(pyS$_4$)}$_2$](I$_3$)$_2$ (22): Black single crystals of **22**·1.8THF that were suitable for X-ray structural analysis were grown from the filtrate after preparation of **10** in the presence of an excess of I_2.

[{Ru(pyS$_4$-Et)}$_2$](BF$_4$)$_2$(B$_2$F$_7$) (23): The single crystals of **23**·3CD_2Cl_2 were obtained during attempts to recrystallize **13** from CD_2Cl_2; spontaneously dealkylation and oxidation of the two Ru centers were observed to occur in the CD_2Cl_2 medium.

[{Ru(pyS$_4$)}$_2$](BF$_4$)(B$_2$F$_7$) (24): The single crystals of **24**·3CH_2Cl_2 were obtained during attempts to recrystallize **13** from CH_2Cl_2; spontaneously dealkylation and oxidation of one of the Ru centers were observed to occur in the CH_2Cl_2 medium.

X-ray Structural Determination of [{Ru(pyS$_4$)}$_2$]·2toluene (4·2toluene), [Ru(NH$_3$)(pyS$_4$)] (6), [Ru(I)(pyS$_4$)]·1.5CH_2Cl_2 (10·1.5CH_2Cl_2), [{Ru(pyS$_4$)}$_2$](PF$_6$)·CD_2Cl_2 (14·CD_2Cl_2), [Ru(NH$_3$)(pyS$_4$)]PF$_6$·CH_2Cl_2 (15·CH_2Cl_2), 0.68[{Ru(pyS$_4$−O$_3$)}$_2$]·0.32[{Ru(pyS$_4$−O$_4$)}$_2$]·2MeOH (0.68 19·0.32 20·2MeOH), [{Ru(pyS$_4$)}$_2$](I$_3$)$_2$·1.8THF (22·1.8THF), [{Ru(pyS$_4$−Et)}$_2$](BF$_4$)$_2$(B$_2$F$_7$)·3CD_2Cl_2 (23·3CD_2Cl_2), and [{Ru(pyS$_4$)}$_2$](BF$_4$)(B$_2$F$_7$)·3CH_2Cl_2 (24·3CH_2Cl_2): Orange rhombs of **4**·2toluene were obtained by recrystallization of a saturated solution of **4** in toluene. Red irregular-shaped crystals of **6** were grown from a saturated H_2O solution of **6**. Black rhombs of **10**·1.5CH_2Cl_2 crystallized from a saturated solution of **10** in CH_2Cl_2. Black blocks of **14**·CD_2Cl_2 were obtained within 10 days from a CD_2Cl_2 solution at room temp. Green fragments of **15**·CH_2Cl_2 formed from a saturated solution of **15** in CH_2Cl_2. Orange prisms of **19/20**·2MeOH formed upon layering a MeOH solution of **19/20** with *n*-hexane. Black crystals of **22**·1.8THF were grown from the filtrate after preparation of **10**. Brown fragments of **23**·3CD_2Cl_2 formed from **13** in a 1:1 mixture of CD_2Cl_2/THF, which was layered with Et_2O. Dark-green platelets of **24**·3CH_2Cl_2 crystallized from a saturated CH_2Cl_2 solution of **13**. Data were collected on a Bruker−Nonius KappaCCD diffractometer using Mo-K_α radiation (λ = 71.073 pm) and a graphite monochromator. Lorentz and polarization corrections were applied for all data sets. A numeric absorption correction was used for **10**·1.5CH_2Cl_2 (Gauss integration).[18] A semiempirical absorption correction has been applied for **14**·CD_2Cl_2 (SORTAV).[19] A semiempirical absorption correction (SADABS)[20] was used for **4**·2toluene, **6**, **15**·CH_2Cl_2, **19/20**·2MeOH, **22**·1.8THF, and **24**·3CH_2Cl_2. All structures were solved by direct methods and refined using full-matrix least-squares procedures on F^2 (SHELXTL NT 6.12).[21] All non-hydrogen atoms were refined anisotropically. The positions of the hydrogen atoms were either taken from the

Table 4. Selected crystallographic data for [{Ru(pyS$_4$)}$_2$] (**4**·2 toluene), [Ru(NH$_3$)(pyS$_4$)] (**6**), and [Ru(I)(pyS$_4$)] (**10**·1.5CH_2Cl_2)

Compound	**4**·2toluene	**6**	**10**·1.5CH_2Cl_2
Formula	$C_{52}H_{46}N_2Ru_2S_8$	$C_{19}H_{18}N_2RuS_4$	$C_{20.5}H_{18}Cl_3INRuS_4$
M_r [g·mol^{-1}]	1157.53	503.66	740.92
Crystal size [mm]	0.14 × 0.10 × 0.05	0.30 × 0.25 × 0.10	0.18 × 0.16 × 0.12
F(000)	588	2032	2880
Crystal system	triclinic	orthorhombic	monoclinic
Space group	$P\bar{1}$	*Pbca*	*C*2/*c*
a [pm]	848.3(1)	1249.9(1)	2163.9(2)
b [pm]	1021.8(1)	1267.8(2)	1366.4(2)
c [pm]	1448.0(2)	2463.9(2)	1763.6(3)
α (°)	103.250(6)	90	90
β (°)	95.209(7)	90	104.626(6)
γ (°)	97.689(6)	90	90
V [nm^3]	1.2011(2)	3.9044(8)	5.0455(9)
Z	1	8	8
$d_{calcd.}$ [g·cm^{-3}]	1.600	1.714	1.951
μ [mm^{-1}]	1.016	1.237	2.505
$T_{min.}/T_{max.}$	0.746/1.000	0.778/1.000	0.602/0.760
Scan technique	ω rotations	φ and ω rotations	φ and ω rotations
2θ Range (°)	6.9−52.8	6.7−56.6	6.8−56.6
Measd. reflections	17246	27662	36368
Indep. reflections	4897	4680	6247
Obsd. reflections[a]	3443	3098	4645
Ref. parameters	290	289	342
*R*1[a]; *wR*2[b] [%]	5.03, 12.73	4.46, 8.94	3.57, 7.28
r_{fin} (max./min.) [e·nm^{-3}]	1.262/−1.199	0.541/−0.542	0.895/−1.046

[a] $[I > 2\sigma(I)]$. [b] All data.

Table 5. Selected crystallographic data for $[\{Ru(pyS_4)\}_2](PF_6)$ (**14**·CD_2Cl_2), $[Ru(NH_3)(pyS_4)]PF_6$ (**15**·CH_2Cl_2), and $0.68[\{Ru(pyS_4{-}O_3)\}_2]\cdot 0.32[\{Ru(pyS_4{-}O_4)\}_2]$ (**19/20**·2MeOH)

Compound	**14**·CD_2Cl_2	**15**·CH_2Cl_2	**19/20**·2MeOH
Formula	$C_{39}H_{30}Cl_2D_2F_6N_2PRu_2S_8$	$C_{20}H_{20}Cl_2F_6N_2PRuS_4$	$C_{40}H_{38}N_2O_{8.64}Ru_2S_8$
M_r [g·mol^{-1}]	1205.16	733.56	1143.58
Crystal size [mm]	0.38 × 0.12 × 0.08	0.23 × 0.15 × 0.07	0.26 × 0.16 × 0.10
F(000)	4792	1460	1154
Crystal system	orthorhombic	monoclinic	monoclinic
Space group	*Ccca*	$P2_1/n$	$P2_1/c$
a [pm]	1663.4(1)	1287.1(1)	1298.2(2)
b [pm]	2381.3(2)	1382.7(2)	1164.9(1)
c [pm]	2287.6(2)	1617.9(2)	1383.8(1)
α (°)	90	90	90
β (°)	90	111.347(5)	102.263(8)
γ (°)	90	90	90
V [nm^3]	9.061(1)	2.6818(6)	2.0449(4)
Z	8	4	2
$d_{calcd.}$ [g·cm^{-3}]	1.764	1.817	1.857
μ [mm^{-1}]	1.247	1.212	1.207
$T_{min.}/T_{max.}$	0.563/0.902	0.631/1.000	0.852/1.000
Scan technique	ω rotations	ω rotations	ω rotations
2θ range (°)	6.7−51.0	6.9−52.0	6.9−51.4
Measd. reflections	38060	21850	30949
Indep. reflectopms	4219	5246	3873
Obsd. reflections[a]	2852	3204	3006
Ref. parameters	286	354	309
$R1$[a]; $wR2$[b] [%]	6.88, 15.10	5.72, 11.44	5.91, 11.97
$r_{fin.}$ (max./min.) [e·nm^{-3}]	0.863/−0.683	0.728/−0.752	0.552/−0.722

[a] [$I > 2\sigma(I)$]. [b] All data.

Table 6. Selected crystallographic data for $[\{Ru(pyS_4)\}_2](I_3)_2$ (**22**·1.8THF), $[\{Ru(pyS_4\text{-}Et)\}_2](BF_4)_2(B_2F_7)$ (**23**·$3CD_2Cl_2$), and $[\{Ru(pyS_4)\}_2](BF_4)(B_2F_7)$ (**24**·$3CH_2Cl_2$)

Compound	**22**·1.8THF	**23**·$3CD_2Cl_2$	**24**·$3CH_2Cl_2$
Formula	$C_{45.2}H_{44.4}I_6N_2O_{1.8}Ru_2S_8$	$C_{45}H_{40}B_4Cl_6D_6F_{15}N_2Ru_2S_8$	$C_{41}H_{36}B_3Cl_6F_{11}N_2Ru_2S_8$
M_r [g·mol^{-1}]	1864.45	1620.4	1469.47
Crystal size [mm]	0.28 × 0.24 × 0.18	0.15 × 0.07 × 0.05	0.24 × 0.19 × 0.06
F(000)	1756	1606	1456
Crystal system	triclinic	monoclinic	triclinic
Space group	$P\bar{1}$	$P2_1/c$	$P\bar{1}$
a [pm]	1405.1(2)	1233.8(1)	1257.8(2)
b [pm]	1429.7(1)	966.1(1)	1320.4(2)
c [pm]	1508.0(2)	2495.5(3)	1666.1(2)
α (°)	73.33(1)	90	92.19(1)
β (°)	70.66(1)	101.66(1)	94.00(1)
γ (°)	79.61(1)	90	103.55(1)
V [nm^3]	2.7261(6)	2.9132(5)	2.6792(7)
Z	2	2	2
$d_{calcd.}$ [g·cm^{-3}]	2.271	1.840	1.821
μ [mm^{-1}]	4.296	1.166	1.248
$T_{min.}/T_{max}$	0.765/1.000	0.790/1.000	0.783/1.000
Scan technique	φ and ω rotations	φ and ω rotations	φ and ω rotations
2θ range (°)	6.9−56.6	6.6−51.4	6.6−56.6
Measd. refl.	50218	29119	52782
Indep. reflections	13340	5409	12322
Obsd. reflections[a]	9437	3370	7677
Ref. parameters	745	426	785
$R1$[a]; $wR2$[b] [%]	3.48, 7.34	5.84, 11.75	4.78, 9.30
r_{fin}(max./min.) [e·nm^{-3}]	2.144/−1.065	0.764/−0.839	0.853/−0.877

[a] [$I > 2\sigma(I)$]. [b] All data.

difference Fourier synthesis and refined with a common isotropic displacement parameter (**6**, **10**·1.5CH_2Cl_2, and **24**·3CH_2Cl_2) or were positioned geometrically with isotropic displacement parameters fixed at 1.2 or 1.5 times the value of *U*(eq) of the preceding carbon atom (**4**·2toluene, **14**·CD_2Cl_2, **15**·CH_2Cl_2, **19/20**·2MeOH, **22**·1.8THF, and **23**·3CD_2Cl_2). Complex **4** crystallized with two toluene molecules per formula unit. Four significant residual electron density maxima are found in close vicinity to the central Ru atom. Complex **10** crystallizes with 1.5 molecules of CH_2Cl_2, which are disordered about the crystallographic inversion center. In the case of **22**·1.8THF, the I_3^- anion is disordered on two alternative sites and the solvate THF molecule is disordered on four different sites. Four significant residual electron density maxima are found in close vicinity of the disordered I_3^-/THF units. The $B_2F_7^-$ anion in the structure of **23**·3CD_2Cl_2 is situated on a crystallographic inversion centre and shares its site with one solvate CD_2Cl_2 molecule, with an occupancy of 50% each. The $B_2F_7^-$ anion in the structure of **24**·3CH_2Cl_2 is disordered on two different sites having occupancies of 78(2)% (for C22, C23) and 22(2)% (for C22′, C23′). The CD_2Cl_2 solvent molecule in **14**·CD_2Cl_2 is disordered on a crystallographic C_2 axis. In the case of **15**·CH_2Cl_2, the CH_2Cl_2 solvate molecule is disordered on two different sites having occupancies of 92.1(4)% and 7.9(4)%, respectively. Two different molecules in **19/20**·2MeOH share a single site on a crystallographic inversion center with occupancies of 68(2)% for [{Ru(pS_4−O_3)}$_2$] (**19**) and 32(2)% for [{Ru(pS_4−O_4)}$_2$] (**20**). The solvate MeOH molecules are also disordered. Selected crystallographic data are summarized in Table 4−6.[22]

Acknowledgments

We thank Prof. Dr. Horst Kisch for valuable discussions of many aspects of this work and the Deutsche Forschungsgemeinschaft (SFB 583 "Redoxaktive Metallkomplexe") for financial support.

[1] D. Sellmann, J. Sutter, *Acc. Chem. Res.* **1997**, *30*, 460−469.
[2] [2a] J. B. Howard, D. C. Rees, *Chem. Rev.* **1996**, *96*, 2965−2982. [2b] B. K. Burgess, D. J. Lowe, *Chem. Rev.* **1996**, *96*, 2983−3012. [2c] R. R. Eady, *Chem. Rev.* **1996**, *96*, 3013−3030.
[3] T. Noguchi, J. Honda, T. Nagamune, H. Sasebe, Y. Inoue, I. Endo, *FEBS Lett.* **1995**, *358*, 50−54.
[4] D. Sellmann, J. Sutter, in *Progr. Inorg. Chem. Dithiolenes in More Complex Ligands* (Eds.: E. I. Stiefel, K. D. Karlin), John Wiley & Sons, Inc., Hoboken, New Jersey **2004**, *52*, chapter 11, 585−681.
[5] [5a] D. Sellmann, W. Soglowek, F. Knoch, G. Ritter, J. Dengler, *Inorg. Chem.* **1992**, *31*, 3711. [5b] D. Sellmann, W. Soglowek, F. Knoch, M. Moll, *Angew. Chem.* **1989**, *101*, 1244; *Angew. Chem. Int. Ed. Engl.* **1989**, *28*, 1271. [5c] D. Sellmann, H. Kunstmann, F. Knoch, M. Moll, *Inorg. Chem.* **1988**, *27*, 4183. [5d] D. Sellmann, T. Hofmann, F. Knoch, *Inorg. Chim. Acta* **1994**, *224*, 61.
[6] D. Sellmann, J. Utz, N. Blum, F. W. Heinemann, *Coord. Chem. Rev.* **1999**, *190−192*, 607−627.
[7] [7a] D. Sellmann, K. Engl, F. W. Heinemann, *Eur. J. Inorg. Chem.* **2000**, 423−429. [7b] D. Sellmann, D. Häußinger, T. Gottschalk-Gaudig, F. W. Heinemann, *Z. Naturforsch.* **2000**, *55*, 723−729. [7c] D. Sellmann, N. Blum, F. W. Heinemann, B. A. Hess, *Chem. Eur. J.* **2001**, *7*, 1874−1880. [7d] D. Sellmann, N. Blum, F. W. Heinemann, *Z. Naturforsch., Teil B* **2001**, *56*, 581−588. [7e] D. Sellmann, J. Utz, F. W. Heinemann, *Inorg. Chem.* **1999**, *38*, 5314−5322.
[8] D. Sellmann, N. Blum, F. W. Heinemann, *Z. Naturforsch., Teil B* **2001**, *56*, 581−588.
[9] D. Sellmann, K. Engl, F. W. Heinemann, J. Sieler, *Eur. J. Inorg. Chem.* **2000**, 1079−1089.
[10] T. Gottschalk-Gaudig, PhD Thesis, University of Erlangen-Nürnberg, **1997**.
[11] D. Sellmann, J. Käppler, M. Moll, F. Knoch, *Inorg. Chem.* **1993**, *32*, 960−964.
[12] [12a] P. G. Douglas, R. D. Feltham, H. G. Metzger, *J. Am. Chem. Soc.* **1971**, *93*, 84. [12b] P. G. Douglas, R. D. Feltham, *J. Am. Chem. Soc.* **1972**, *94*, 5254.
[13] D. Sellmann, T. Gottschalk-Gaudig, F. W. Heinemann, *Inorg. Chimica Acta* **1998**, *269*, 63−72.
[14] [14a] R. M. Buonomo, I. Font, M. J. Maguire, J. H. Reibenspies, T. Tuntulani, M. Y. Darensbourg, *J. Am. Chem. Soc.* **1995**, *117*, 963. [14b] S. A. Mirza, M. A. Pressler, M. Kumar, R. O. Day, M. J. Maroney, *Inorg. Chem.* **1993**, *32*, 977.
[15] [15a] L. A. Tyler, J. C. Noveron, M. M. Olmstead, P. K. Mascharak, *Inorg. Chem.* **1999**, *38*, 616−617, [15b] L. A. Tyler, J. C. Noveron, M. M. Olmstead, P. K. Mascharak, *Inorg. Chem.* **2000**, *39*, 357−362. [15c] J. C. Noveron, M. M. Olmstead, P. K. Mascharak, *Inorg. Chem.* **2001**, *123*, 3247−3259.
[16] [16a] G. N. Schrauzer, C. Zhang, R. Chadha, *Inorg. Chem.* **1990**, *29*, 4104−4107. [16b] C. A. Grapperhaus, M. Y. Darensbourg, *Acc. Chem. Res.* **1998**, *31*, 451−459.
[17] M. Koepp, H. Wendt, H. Strehlow, *Z. Elektrochem.* **1960**, *64*, 483.
[18] P. Coppens, in *Crystallographic Computing* (Eds.: F. R. Ahmed, S. R.Hall, C. P. Huber), Munksgaard, Copenhagen, **1970**, pp. 255−270.
[19] R. H. Blessing, *Acta Crystallogr., Sect. A* **1995**, *51*, 33−38.
[20] SADABS, Bruker-Nonius, Inc., **2002**, Madison, WI, USA.
[21] SHELXTL NT 6.12, Bruker AXS, Inc., **2002**, Madison, WI, USA.
[22] CCDC-229802 (for **4**·2toluene), -229803 (for **6**), -229804 (for **10**·1.5 CH_2Cl_2), -229805 (for **14**·CD_2Cl_2), -229806 (for **15**·CH_2Cl_2), -229807 (for **19/20**·2 MeOH), -229808 (for **22**·1.8 THF), -229809 (for **23**·3 CD_2Cl_2), and -229810 (for **24**·3 CH_2Cl_2)contain the supplementary crystallographic data for this paper. These data can be obtained free of charge at www.ccdc.cam.ac.uk/const/retrieving.html [or from the Cambridge Crystallographic Data Centre, 12 Union Road, Cambridge CB2 1EZ, UK; Fax: (internat.) + 44-1223/336-033; E-mail: deposit@ccdc.cam.ac.uk.

Received January 27, 2004
Early View Article
Published Online May 27, 2004

